UV radiation sensors with unitary and binary superficial barrier

Dorogan, Valerian, Vieru, Tatiana, Kosyak, V., Damaskin, I., Chirita, F.

Valerian Dorogan, Tatiana Vieru, V. Kosyak, I. Damaskin, F. Chirita, "UV radiation sensors with unitary and binary superficial barrier," Proc. SPIE 3405, ROMOPTO '97: Fifth Conference on Optics, (2 July 1998); doi: 10.1117/12.312705

SPIE.

Event: ROMOPTO '97: Fifth Conference on Optics, 1997, Bucharest, Romania

UV radiation sensors with unitary and binary superficial barrier

V.Dorogan, T.Vieru, V.Kosyak, I.Damaskin*, F.Chirita

Laboratory of Microelectronics, Technical University of Moldova,
bd. Stefan cel Mare 168, MD 2012 Kishinev, Moldova
*Institute of Applied Physics, Academy of Sciences of Moldova,
str. Academiei 5, MD 2028 Kishinev, Moldova

ABSTRACT

UV radiation sensors with unitary and binary superficial barrier, made on the basis of GaP - SnO_2 and GaAs - AlGaAs - SnO_2 heterostructures, are presented in the paper. Technological and constructive factors, whici permit to realize a high conversion efficiency and to exclude the influence of visible spectrum upon the photoanswer, are analysed. It was established that the presence of an isotypical superficial potential barrier permits to suppress the photoanswer component formed by absorption of visible and infrared radiation in semiconductor structure bulk.

Keywords: Ultraviolet radiation sensor, heterostructures, A^3B^5 compounds, superficial potential barrier.

1. INTRODUCTION

The conversion efficiency and spectral sensibility of UV radiation sensors are determined by many factors, the most important being the band gap of utilized semiconductors. Fot the UV region the most perspective materials are semiconductors with band gap $E_g > 2.5$ eV ($\lambda < 0.49$ μm). Moreover, we have to consider the material reflection and refraction coefficients for $\lambda < 0.49$ μm, the defect density in potential barrier region, condition of structure surface. At present, the following semiconductor materials are utilized for UV sensors manufacturing: Si, A^3B^5 compounds and their solid solutions, A^2B^6 compounds, SiC etc.

The UV sensors need a high separating efficiency of charge carriers photogenerated by UV radiation at structure surface. Therefore, a small density of surface energetic states and presence of superficial potential barrier are required. The most spread are structures on the basis of p-n junction, Schottky barrier and on the basis of heterostructures with optic window.

Because Si is the most used semiconductor, sensors on the basis of single-crystal Si with superficial p-n junction (depth ~ 0.1 μm) and on the basis of MOS structures were realized. But in both cases the photosensibility maximum is placed in near IR spectral region.[1]

More efficient are the structures with Au - GaAs Schottky barrier.[2] Their photosensibility spectrum has maximum for photons $h\nu \approx 2.5$ eV and external efficiency $\eta_e = 40$ % in photosensibility maximum.

The other way to extend the photosensibility spectrum in UV region is utilization of Au - $nGaAs_{0.6}P_{0.4}$ structures, on the basis of which an efficiency of 40 % was obtained for photons $h\nu = 3.5$ eV ($\lambda = 0.36$ μm).[3]

$Ga_{1-x}Al_xP$ ternary compounds permit to move the photosensibility red boundary up to 3.1 eV. The quantum efficiency of Au - $nGa_{1-x}Al_xP$ ($x = 0.5 \pm 0.1$) - nGaP structures is 30 %.[4]

The structures with superficial barrier on the basis of GaP ($E_g = 2.27$ eV) are also intensive investigated. To form the Schottky barrier the following metals are used here: Au, Pt, Ni, Mo, Al, Cr, Ag, Cu, Mg. The potential barrier height varies from $\varphi = 1.13$ eV (for Mo - GaP) to $\varphi = 1.45$ eV (for Pt - GaP, Au - GaP) and depends on GaP surface quality and on metal deposition method.[5] Au - GaP structure is the most studied and the most effective. The separating efficiency of charge carriers is 45 % for photons $h\nu = 3.3$ eV.[6]

GaP - In_2O_3, GaP - SnO_2 and GaP - ITO structures are also studied. Sensors on nGaP - n^+GaP epitaxial structures with charge carriers concentration $n \approx 10^{16}$ cm^{-3} and $\mu_n = 70$ - 120 $cm^2 \cdot V^{-1} \cdot s^{-1}$ have an absolute monochromatic sensibility of 1.5 times more than of Au - GaP sensors fabricated by Hamamatsu firm.[7,8]

2. RESULTS AND DISCUSSION

The results in manufacturing the UV sensors on the basis of GaP - SnO_2 and GaAs - AlGaAs - SnO_2 heterostructures are presented in this paper.

n(p)-GaP with crystallographic orientation (111) was utilized as a substrate to prepare GaP - SnO_2 structures (Fig.1). Concentration of free charge carriers was n(p) = 10^{17} - 10^{18} cm^{-3}. The back ohmic contact was formed by electrolytic deposition of Ni. Current density in electrolyte was j = 5 - 10 mA/cm^2. To reduce the contact resistance, substrates were heated in hydrogen at T = 600 - 650 °C for 1-2 minutes. The frontal contact was formed by vacuum thermal deposition of metals and consisted of two layers (Ni + Cu).

SnO_2 layer was formed by two methods:

a) Pyrolysis from gas phase of tin acetylacetonate transported by a warm air flux. Temperature of heater was + 200 °C. GaP substrate temperature varied in interval 360 - 450 °C. Process duration was 30 - 60 min.

b) Multiple deposition (~ 10 times) of SnO_2 thin films by spraying and following pyrolysis of tin chloride solution in ethylic spirits. Substrate temperature was ~ 400 °C. One process duration - 3 min.

To improve the potential barrier properties we had utilized the epitaxial forming of crystalline films, which have more less structural defects and mechanical strains than initial GaP substrate. GaP epitaxial layers were formed on n-GaP, p-GaP, i-GaP (111) substrates by liquid phase epitaxy in temperature interval 800 - 950 °C.

The other way to form GaP - SnO_2 structures with high quality potential barrier is to reduce the concentration of noncontrolled dope impurities (background concentration). The melts was doped with rare elements (Er and Y) to reduce the concentration of electric active impurities in GaP epitaxial layers.

The concentration of free charge carriers in epitaxial layers was determined by Hall method. Epitaxial layers without rare elements have a background concentration $n = 5 \cdot 10^{16} - 6 \cdot 10^{17}$ cm^{-3} and a mobility of free charge carriers $\mu = 20 - 60$ $cm^2 \cdot V^{-1} \cdot s^{-1}$.

The presence of erbium (Er) in Ga + P melt causes an irregular growth of epitaxial layer with bad morphology.

Itrium (Y) has a more positive influence. The presence of 0.2 - 0.5 mg of Y in one gramme of melt and multiple utilization of melt reduce the concentration of electric active impurities in solid phase up to $n = 3.5 \cdot 10^{15}$ cm^{-3}. Moreover, in such mode we can invert the conductivity type (from **n** into **p**). Maximal mobility of free electrons is $\mu = 100$ $cm^2 \cdot V^{-1} \cdot s^{-1}$ for charge carriers concentration $n = (3\text{-}6) \cdot 10^{16}$ cm^{-3}.

The influence of melt thermocycling with and without itrium upon the concentration of electric active impurities in epitaxial layer is presented in Fig.2.

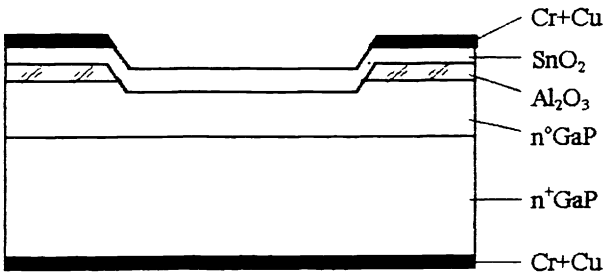

Fig.1. Structure of UV radiation sensor.

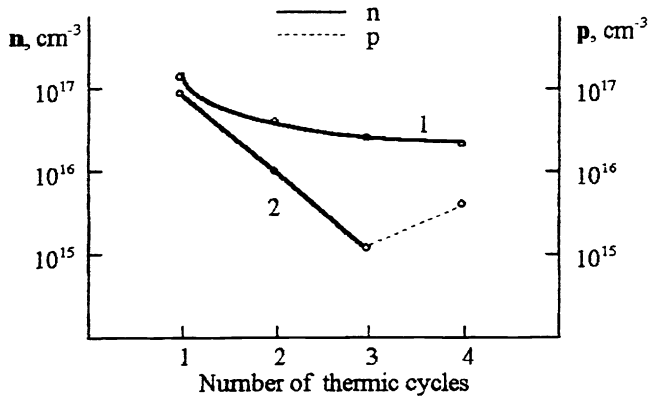

Fig.2. Charge carriers concentration in dependence of melt thermocycling: 1 - without itrium; 2 - with itrium.

Thus, the optimum parameters of epitaxial layers were obtained using the Ga + P melt with rare elements (Y) and heating them after a special regime. During the heating the melt was homogenized (uniform distribution of P and Y in Ga). At cooling itrium formed with impurities any inactive compounds decreasing so their concentration in solid phase.

After epitaxial structure forming an Al_2O_3 layer was deposited on the frontal surface to limit the area of potential barrier which appears at GaP - SnO_2 interface. Windows with diameter 400 μm were opened in Al_2O_3 layer by photolitography.

2.1. Spectral characteristics.

Spectral characteristics of UV sensors with pGaP - nSnO_2 structure are presented in Fig.3. nSnO_2 layer was made here by pyrolysis of tin acetylacetonate. Curves "a" and "b" represent the photoanswer measured in constant flux regime and in impulse regime (frequency 38 Hz) respectively. Curve "c" is the spectral photoanswer reported to spectrum of radiation source (lamp ДКСШ-200). One can see that photosensibility interval, determined at level 0.1 of maximal value, is 0.37 - 0.49 μm. Comparing the spectral sensibility of pGaP - nSnO_2 structure with that of pGaP - electrolyte barrier (Fig.4) in interval 0.3 - 0.49 μm, we established that photoanswer is formed by charge carriers generated in GaP semiconductor crystal. The abrupt decreasing of photosensibility for wavelengths $\lambda < 0.36$ μm is caused by absorption of radiation in SnO_2 layer, by generation of charge carriers and by their recombination in the bulk or on the surface of SnO_2 layer (with thickness of 150 nm).

The spectral photoanswer of "electrolyte - SnO_2 - GaP" structure (Fig.5) was measured to show that high recombination velocity of charge carriers in SnO_2 layer causes the practically zero sensibility in spectral region $\lambda < 0.36$ μm.

The maximum at 320 nm (SnO_2 band gap is 3.6 - 3.8 eV) is caused by charge carriers photogenerated in SnO_2 layer. Low intensity of this maximum demonstrates the small weight of generated in SnO_2 layer charge carriers in sensor's photocurrent forming. Cause can be only the imperfect structure of SnO_2 layer made on the basis of non-optimized technology.

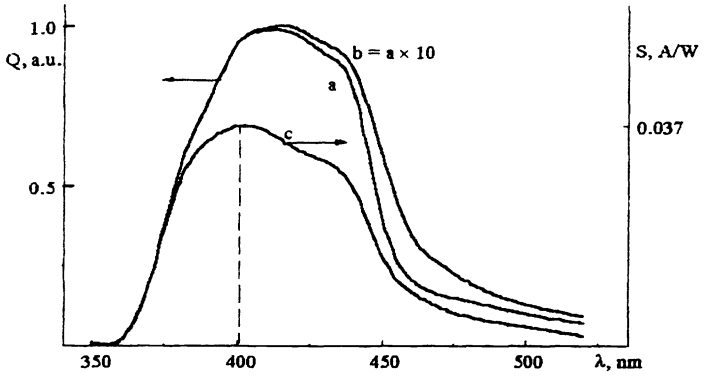

Fig.3. Spectral characteristics of pGaP - nSnO₂ structure: a - in constant flux regime; b - in impulse regime; c - "a" reported to spectrum of radiation source.

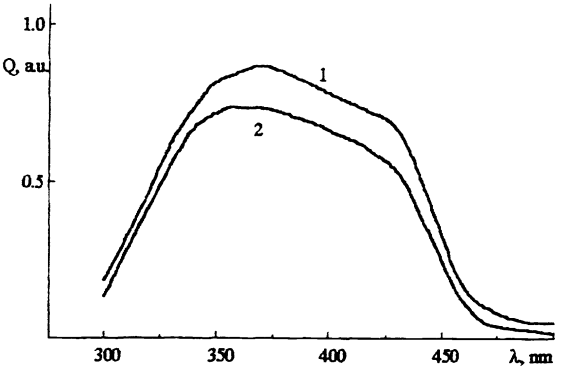

Fig.4. Spectral characteristics of GaP - electrolyte structure: 1 - nGaP; 2 - pGaP.

Fig.6 shows the measured photoanswer spectrum (curve 1) of nGaP - nSnO₂ structure, emission spectrum of lamp ДКСШ-200 (curve 2) and spectral photoanswer reported to emission spectrum of lamp, so the spectral sensibility of structure (curve 3). The photosensibility interval extends here after 0.26 μm.

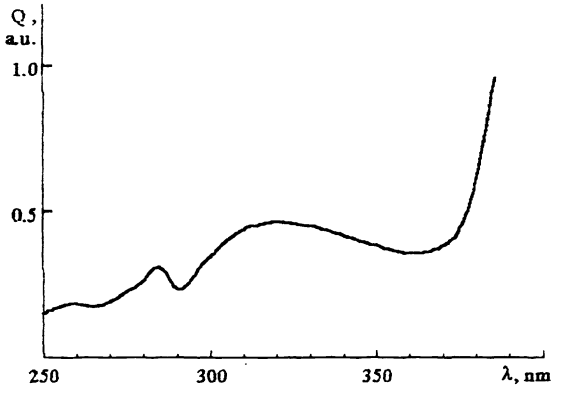

Fig.5. Spectral characteristic of "electrolyte - SnO₂ - GaP" structure.

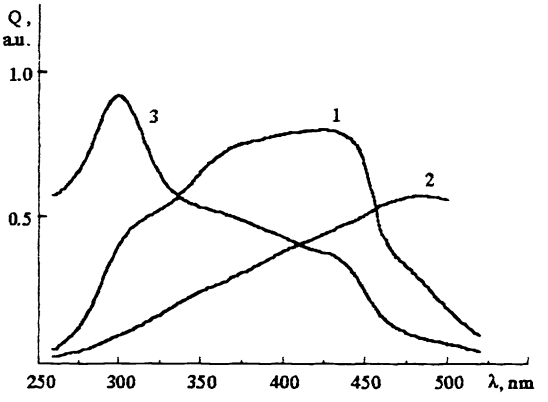

Fig.6. Spectral characteristics of nGaP - nSnO₂ structure: 1 - measured; 2 - emission spectrum of lamp; 3 - measured spectrum reported to lamp spectrum.

Because of absence of a radiation source with wavelengths $\lambda < 0.26$ μm, we could not determine the left side of photosensibility (on the wavelength scale), but we had established that the contribution of SnO_2 layer in photocurrent forming is more than GaP substrate's one. This demonstrates that one must give an exclusive attention to manufacturing technology of SnO_2 films to obtain a major sensibility in UV region.

2.2. Kinetics of photocurrent forming and relaxation.

Manufactured and studied GaP - SnO_2 structures are characterized by big times of photocurrent forming and relaxation. Fig.7 illustrates the form of incident flux impulse (a) and the photocurrent form (b) determined by stroboscopic oscilloscope for photovoltaic regime. In initial moment t_1 the photocurrent increases abruptly up to its maximal value I_1. During the 5 - 10 ms the photocurrent intensity decreases to $I_1/e = 0.37 \cdot I_1$ forming its stationary value I_{st}. After incident photoimpulse finishing, in the moment t_2, the photocurrent changes suddenly its direction taking the value $-I_2$ and relaxes exponential. The ratio of photocurrents in positive and negative maximum to stationary photocurrent is: $I_1/I_{st} = 5\text{-}6$; $I_2/I_{st} = 3\text{-}4$. External quantum efficiency in impulse regime in photosensibility maximum is about 50 - 60 %.

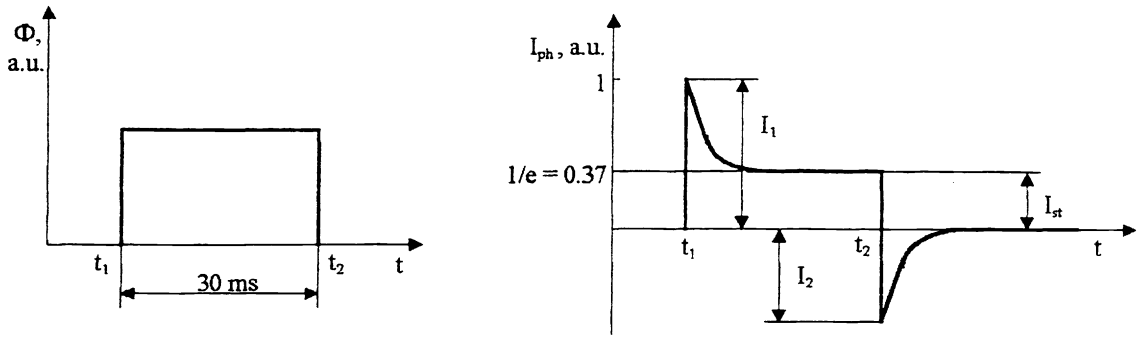

Fig.7. Incident radiation impulse and the form of sensor photoanswer.

The photoanswer kinetics can be appreciate using [9,10]. In structures with intermediate dielectric layer the photocurrent forming is determined by two processes: by loading the structure capacity and by tunnel current through dielectric layer between GaP substrate and SnO_2 layer. The photocurrent kinetics is determined by relation:

$$I_{ph}(t) = q \cdot I \cdot \left[\frac{C_d}{C_d + C_{sc}} \cdot e^{-t/\tau} + \frac{S_{em}}{S_{em} + S_{rec}} \cdot \left(1 - e^{-t/\tau}\right) \right], \quad \text{for } t_1 < t < t_2$$

$$I_{ph}(t) = q \cdot I \cdot \left(\frac{S_{em}}{S_{em} + S_{rec}} - \frac{C_d}{C_d + C_{sc}} \right) \cdot e^{-t/\tau}, \quad \text{for } t > t_2$$

where: I_{ph} - photocurrent density;

I - flux of charge carriers generated in semiconductor;

C_d, C_{sc} - specific capacity (to a surface unit) of dielectric layer and of space charge region in semiconductor;

S_{em}, S_{rec} - effective velocity of charge carriers emission from semiconductor to SnO_2 layer and summary velocity of charge carriers recombination.

τ - time constant.

In dependence of parameters S_{em}, S_{rec}, C_d and C_{sc} a lot of relaxation variants are possible.

Let analyse the case $S_{em} < S_{rec}$. For $C_d > C_{sc}$ the photocurrent relaxation, according to relation $I_{ph}(t)$, has different directions. At the beginning of incident flux impulse the photocurrent increases quickly up to value qI, then relaxes to its stationary value $q \cdot I \cdot S_{em}/S_{rec}$ with time constant τ. At the photoimpulse end ($t > t_2$) the photocurrent changes its direction.

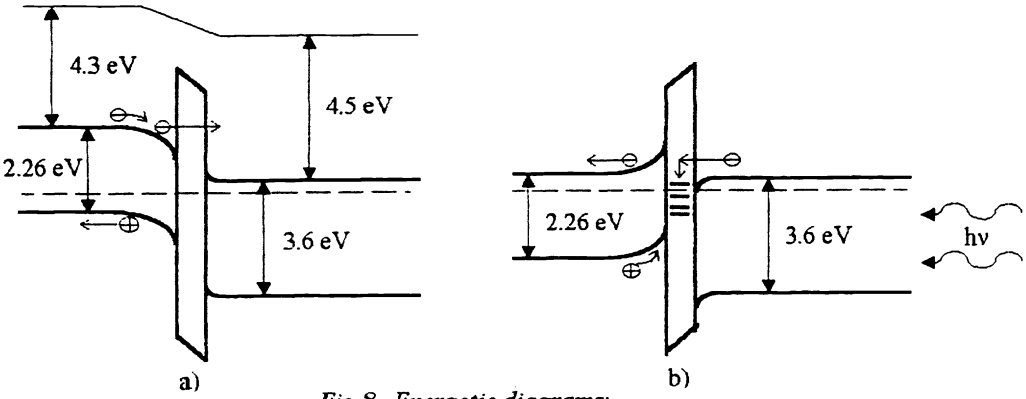

Fig.8. Energetic diagrams:
a - pGaP - nSnO₂ structure; b - nGaP - nSnO₂ structure.

To better understanding the mechanism of photocurrent forming we had constructed the energetic diagrams of pGaP - $nSnO_2$ and nGaP - $nSnO_2$ structures with intermediate dielectric layer (Fig.8). In photocurrent impulse forming a considerable contribution is given by the transition of excessive minority charge carriers from GaP semiconductor through oxide layer to SnO_2 one. The presence of potential pits at semiconductor interface leads to accumulation in them of charge carriers whose concentration depends on dielectric layer transparency (that is on its thickness) and on dielectric constant ε. Thus, in the first moment t_1 the structure capacity is loading. At structure's reverse polarisation the layer transparency increases and the ratio I_1/I_{st} decreases. At direct polarisation the structure photocurrent decreases, what demonstrates the

presence of a big differential resistance. Cause is the increasing of potential barrier effective thickness for photogenerated minority electrons.

2.3. Volt-amper characteristics.

Volt-amper characteristics (VAC) in dark and light conditions are presented in Fig.9. VAC measured in temperature interval -5 ÷ +80 °C have the same abruptness. It is characteristic for tunnel mechanism of the current through heterojunction.

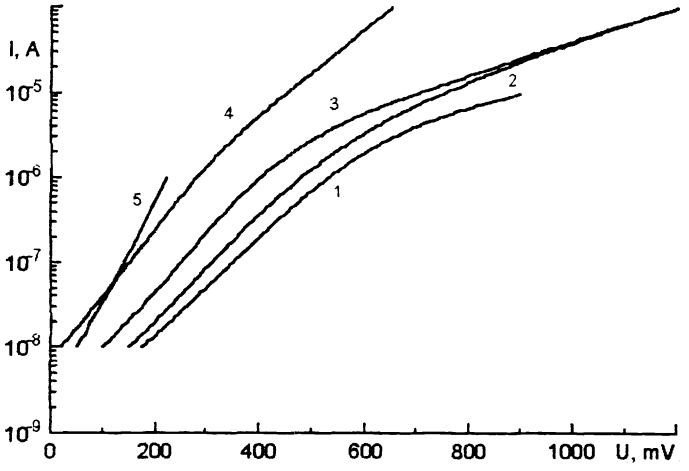

Fig.9. Volt-amper characteristics:
1-4 - in dark, n = 2.15; T, °C: 1 - 0; 2 - 12; 3 - 20; 4 - 70; 5 - at illumination, n = 1.33.

Curve 5 represents the dependence $I_{sc} = f(U_{oc})$ constructed on the basis of characteristics I_{sc}, $U_{oc} = f(E)$. One can observe that VAC nonideality coefficient in dark conditions (n = 2.15) differs from that in light conditions (n = 1.33). It means that in studied structures the superposition principle, according to which injection current and photocurrent have the same forming mechanism, isn't fulfilled.

Effected investigations showed that GaP - SnO_2 structures can be successfully used for UV radiation sensors manufacturing. The following conditions are required to improve the conversion efficiency of optic radiation:

- An epitaxial layer with thickness d > 5 μm have to be formed on GaP substrate to reduce considerable the density of superficial defects.
- To ensure the concentration of electric active impurities at level 10^{16} cm^{-3}, the epitaxial layer is growing from doped with rare elements liquid phase.
- The SnO_2 layer forming technology must exclude the forming on GaP substrate of an oxide layer, which determines the structure's total capacity.
- To reduce considerable the superficial recombination velocity of charge carriers, the potential barrier at semiconductors interface must be tunnel transparent.
- A superficial isotypical barrier for minority carriers from GaP has to be formed to reduce the contribution of charge carriers generated by photons with $h\nu \approx E_g^{GaP}$.

To exclude the influence of absorbed in semiconductor bulk radiation and to register only the charge carriers generated at surface by high energy photons, we realized a nGaAs - $n^+Al_{0.85}Ga_{0.15}As$ - own oxide - SnO_2 structure with binary superficial barrier (fig.10). The $n^+Al_{0.85}Ga_{0.15}As$ layer with band gap $E_g \approx 2.1$ eV was grown on nGaAs substrate by liquid phase epitaxy. The concentration of free charge carriers changed in interval $4 \cdot 10^{17} \div 3 \cdot 10^{19}$ cm^{-3} and the layer thickness varied within limits 0.1 ÷ 10 μm. The space charge region with thickness W was localized at AlGaAs-SnO_2 interface. SnO_2 layer thickness didn't exceed 100 nm. An anodic oxide thin layer, tunnel transparent, was formed on the epitaxial layer to decrease the superficial states density.

The photons, absorbed at AlGaAs layer surface, generate charge carriers in excess, which are separated by AlGaAs-SnO_2 potential barrier. The charge carriers generated in the AlGaAs layer are similar separated. For holes generated in GaAs substrate there is a potential barrier, which brakes their diffusion to internal electric field of space charge region. Thus, the carriers generated in nGaAs substrate recombine without any contribution in photocurrent forming.

The separation coefficient of charge carriers Q depending on incident photons energy for different thicknesses of AlGaAs layer (d_{AlGaAs}) and of space charge region (W) is presented in fig.11. One can see that Q is maximal in interval $2.1 < h\nu < 4.4$ when d_{AlGaAs} and W have maximal values. The coefficient Q decreases non-uniform with d_{AlGaAs} and W decreasing:

quickly for low energies and slowly for high ones. It is due to absorption coefficient α, which decreases concomitent with photons energy. Particular is the second case, when the space charge region begins to extend also in nGaAs substrate, extracting the excessive carriers.

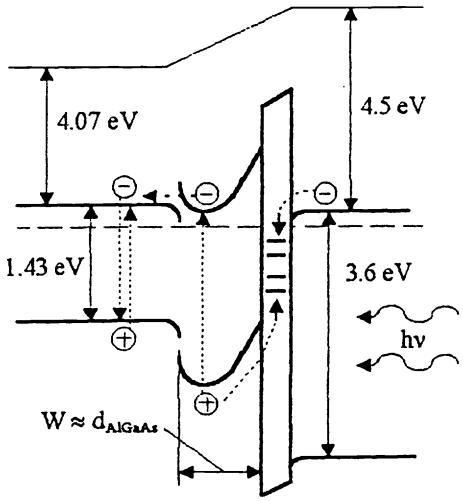

Fig.10. Energy diagram of the structure with binary superficial barrier.

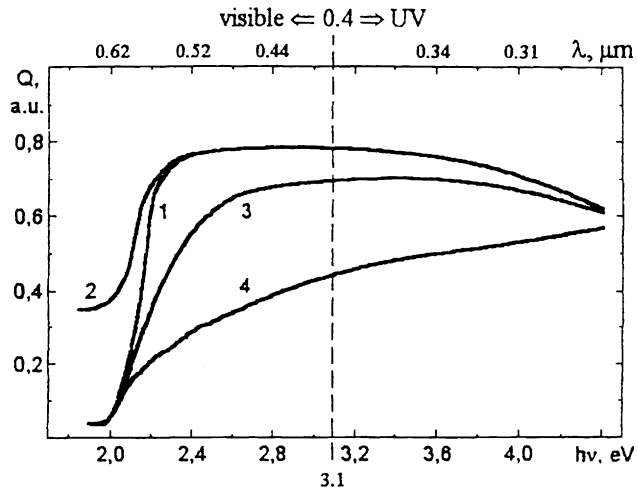

Fig.11. Spectral dependence of separation coefficient: 1 - $d_{AlGaAs} > W = 1$ μm; 2 - $d_{AlGaAs} \approx W = 1$ μm; 3 - $d_{AlGaAs} \geq W = 0.5$ μm; 4 - $d_{AlGaAs} \geq W = 0.1$ μm.

Thus, varying the band gap width of AlGaAs frontal layer, its doping level and the thickness of AlGaAs layer, in which th space charge region is localized, we can change the structure sensibility to different energy photons. Even if some semiconductors with nonoptimized band gap less than threshold energy of UV region (hν = 3.1 eV) are utilized, a photosensibility with visible component less than UV one can be realized (fig.11, curve 4). It was determined that the conversion efficiency of UV photons depends on perfection of AlGaAs-SnO_2 heterojunction, on intensity of barrier internal field which separates the photogenerated carriers, on thickness and transparency of SnO_2 layer. The visible component can be suppressed by realizing a structure in which the photons with energy hν < 3.1 eV are absorbed in a region with potential barrier, which brakes the excessive carriers separation.

3. REFERENCES

1. L. E. Klyachkin, L.B. Lopatina, A.M. Malyarenko, V.L. Suhanov, "Spektralnye harakteristiki selektivnyh FP dlya vidimoi i UF oblastei spektra", *Pisma v JTF* **11**(6), 354-356 (1985).

2. A. A. Gutkin, M. V. Dmitriev, D. N. Nasledov, A. V. Pashkovski, "Spektry fotochuvstvitelnosti poverhnstno-bariernogo dioda Au-nGaAs v oblasti energii fotonov 1-5 eV", *FTP* 5(10),1927-1933 (1971).

3. A. Berkeliev, Yu. A. Goldberg, D. Melevaev, B. V.Tsarenkov, "FP vidimogo i UF izlucheniya na osnove $GaAs_{1-x}P_x$ poverhnstno-bariernyh struktur", *FTP* **10**(8),1532-1538 (1976).

4. A. R. Annaeva, A. Berkeliev, V. N. Bessolov, Yu. A. Goldberg, B. V.Tsarenkov, Yu. P.Yakovlev, "FP UF izlucheniya na osnove varizonnoi $Ga_{1-x}Al_xP$ (X_v = 0.5+0.1) poverhnstno-bariernoi struktury", *FTP* **15**(6),1122 (1981).

5. T. F. Lei, L. Lee Chung, C. Y. Chang, "Metal-nGaP Schottky barrier heights", *Sol. St. Electron.* **22**(12),1035-1037 (1979).

6. B. V.Tsarenkov, G. V. Gusev, Yu. A. Goldberg, "Fotoelektricheskie svoistva poverhnstno-bariernyh struktur v UF polose spektra", *FTP* **8**(2),410-416 (1974).

7. A. I. Malik, G. G. Grushka, "Optoelektronnye svoistva geteroperehodov okisel metala GaP", *FTP* **25**(11),1691-1696 (1991).

8. A. I. Malik, V. A. Grechiko, V. E. Anikin, "Porogovie priemniki korotkovolnovogo izlucheniya na osnove diodov Schottky A^3B^5", *JTF* **59**(11),104-107 (1989).

9. O. Yu. Borkovskaya, A. T. Voroshenko, I. D. Dmitruk, A. K. Erohin, O. N. Mishchuk, "Fotoelektricheskie svoistva geteroperehoda IT/GaAs", *Optoelektronika i poluprovodnikovaya tehnika* **18**,97-100 (1990).

10. A. Ya. Vul, A. G. Dideikin, Yu. S. Zinchik, K. V. Sanin, A. V. Sachenko, "Kinetika fotootveta tunnelnyh MDP struktur", *FTP* **17**(8),1471-1477 (1983).